

Experimental investigation of the surface acoustic wave electron capture mechanism

M. Kataoka, C. H. W. Barnes, H. E. Beere, D. A. Ritchie, and M. Pepper
Cavendish Laboratory, Madingley Road, Cambridge CB3 0HE, United Kingdom

(Received 27 March 2006; revised manuscript received 24 May 2006; published 1 August 2006)

We have investigated surface acoustic wave charge transport through a one-dimensional channel, where the form of the potential is defined by two split gates placed in series. It is found that, when the second gate is set to shut off the acoustoelectric current, sweeping the first gate to negative voltages recovers the current and a set of current-quantization plateaux are observed. At a certain negative gate voltage, a sudden transition occurs and the current starts to decrease to zero, again showing plateaux. Calculation of the channel potential shows that this counterintuitive behavior is caused by the switching of maximum potential slope between two different locations that give different current dependencies. This result indicates that in the high transducer-power regime, the charge transport by surface acoustic wave is determined by the potential gradients.

DOI: [10.1103/PhysRevB.74.085302](https://doi.org/10.1103/PhysRevB.74.085302)

PACS number(s): 73.23.Hk, 73.50.Rb, 73.63.Kv

It has been demonstrated that surface acoustic waves (SAWs) on a GaAs/AlGaAs heterostructure can transport a single electron in each moving potential minimum, resulting in the quantisation of the acoustoelectric current.¹ A SAW is generated by applying microwave power to an interdigitated transducer fabricated on a GaAs surface. Owing to the piezoelectric properties of GaAs, the SAW is accompanied by a moving electrical potential modulation. Along the traveling direction of the SAW, a narrow depleted channel is placed between source and drain two-dimensional electron gases (2DEGs). As the traveling potential waves pass along the channel, electrons in the source 2DEG are caught in the potential minima and are carried to the drain 2DEG, driving the acoustoelectric current. By adjusting the potential of the channel, the average number n of electrons in each minimum can be tuned so that the current through the channel is quantized at nef , where f is the SAW frequency.

Progress in using SAWs to make either a type of current standard² or a dynamic quantum processor^{3,4} have been slowed partly because the exact mechanism for current quantization is not fully understood. Existing models explain the electron capture mechanism in different ways.⁵⁻⁹ The most significant difference is that, whereas Flensberg *et al.*⁵ and Maksym⁶ consider the electron depopulation mechanism at equilibrium with the source 2DEG, in the models by Aizin *et al.*,^{7,8} and Robinson and Barnes,⁹ the electrons are transported through the channel out of equilibrium. In these out-of-equilibrium models, the electrons captured at the entrance of the channel escape through the barrier between the SAW dot and the source 2DEG either by tunneling^{7,8} or by thermal excitation.⁹ In Refs. 7 and 8 the final number of electrons transported depends on the time integral of the tunneling probability through the barrier. In Ref. 9, the number is determined by the point where the barrier is weakest, or where the potential gradient in the transport direction is maximum.

Moreover, recent experimental work by Fletcher *et al.*¹⁰ suggests that none of these pictures may be the real mechanism. They found that, as the SAW amplitude was incremented, current-quantization plateaux developed from Coulomb-blockade oscillations observed without the presence of a SAW (by dc measurements). It was proposed that the current quantization is caused by a turnstile motion of a quantum dot¹¹ unintentionally created by an impurity poten-

tial. In their picture, the SAW modulates the potential of the entrance and exit tunneling barriers and the dot itself, and hence allows electrons to travel through the dot. The current is determined by the addition energy of the dot, which determines the number of electrons allowed to pass through the dot simultaneously with a given SAW amplitude. If such turnstile motion is the main mechanism of the current quantization, then electron transport through long channels will be difficult because of randomly placed tunnel barriers due to impurity potential, thereby effectively preventing the application of SAWs to quantum information technology.^{3,4}

With this as a motivation we have studied SAW electron transport through a channel defined by two split gates placed in series. The gates are closely spaced so that, when sufficient voltages are applied, a single long depleted channel is expected to form. As a gate voltage is swept, the acoustoelectric current shows a triangular-shaped peak with current-quantization plateaux on both sides. This peculiar behavior is explained by considering that the current is limited by the maximum electric field that minimizes the SAW confinement potential, as expected in the classical picture given by Robinson and Barnes.⁹ The position of the maximum field switches between two different locations as the gate voltages are varied, resulting in a sharp peak in the current. We compare the experimental data with the potential calculated by solving the three-dimensional Laplace's equation, and discuss that it is unlikely that a quantum dot in the channel¹⁰ can cause such a behavior.

The sample was fabricated from a GaAs/AlGaAs heterostructure containing a 2DEG situated 90 nm below the surface with a sheet density $1.5 \times 10^{15} \text{ m}^{-2}$ and mobility $50 \text{ m}^2/\text{V s}$. Metals (20 nm Ti and 40 nm Al) for a SAW interdigitated transducer with 70 pairs of fingers and Schottky gates (schematically shown as G1, G2, and G3 in Fig. 1) were patterned by electron-beam lithography. The widths of gates G1 and G2 are both $0.7 \mu\text{m}$, and the separation between them is $0.3 \mu\text{m}$. The gaps between G1/G2 and G3 are both $0.8 \mu\text{m}$. The lithographic period of the transducer fingers is $1.0 \mu\text{m}$, and the resonant frequency is 2.706 GHz at 1.2 K. The distance between the transducer and the device is roughly 2.5 mm. There is approximately 6 dB attenuation on the coaxial line between the radio-frequency source (a signal generator) and the transducer. The

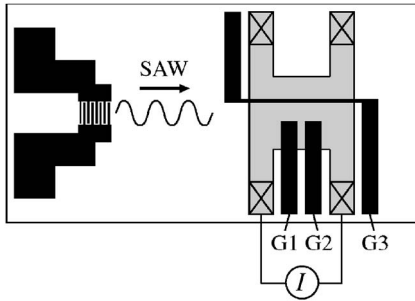


FIG. 1. A schematic diagram of the sample. The interdigitated transducer on the left produces a SAW running towards the mesa on the right (shown in gray) containing a 2DEG. The lithographic length of the channel defined by gates G1, G2, and G3 is approximately $1.7 \mu\text{m}$. The current through the channel is measured from the ohmic contacts shown as crossed boxes.

power, P , quoted in this paper is the output power of the source. We note that because of impedance mismatch, most of the power incident on the transducer is reflected back to the source. Measurements were performed at 1.2 K.

The inset to Fig. 2 shows the acoustoelectric current, I , measured as a function of the voltage on G1 (V_{G1}). The voltages on G2 and G3 (V_{G2} and V_{G3}) are fixed at 0 V and -2.4 V, respectively. The transducer power is $P=13.5$ dBm. The nonzero current at $V_{G1}=0$ V is due to the offset voltage of the current preamplifier, which is around $150 \mu\text{V}$.¹² The data near the pinch off are shown in the leftmost curve in the main figure of Fig. 2, showing at least three current-quantization plateaux ($ef=0.434$ nA). This figure also shows a series of curves as V_{G2} is decremented from 0 to -1.4 V in 0.05 V steps (no offset is applied to the curves). Initially, the curves shift towards positive V_{G1} as V_{G2} is decreased from zero. This can be simply interpreted as that G1 requires a smaller negative voltage to pinch off the chan-

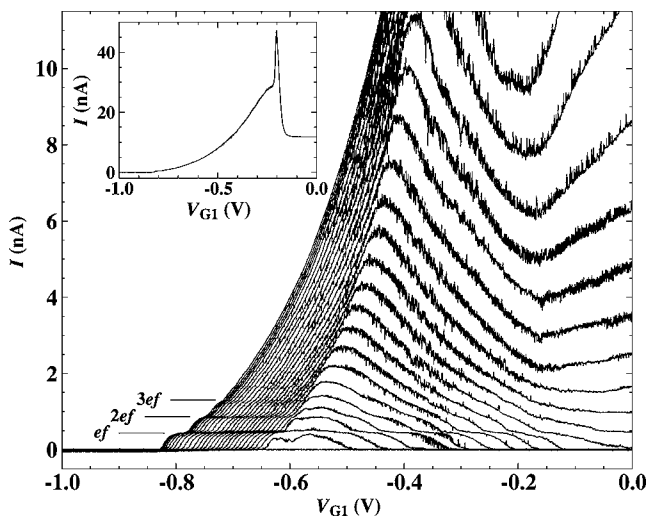


FIG. 2. Acoustoelectric current, I , as a function of the voltage on G1, V_{G1} . The voltage on G2, V_{G2} , is decremented from 0 V (on the leftmost curve) to -1.4 V by 0.05 V step. The inset shows the I - V_{G1} curve when $V_{G2}=0$ V. The power on the transducer is $P=13.5$ dBm.

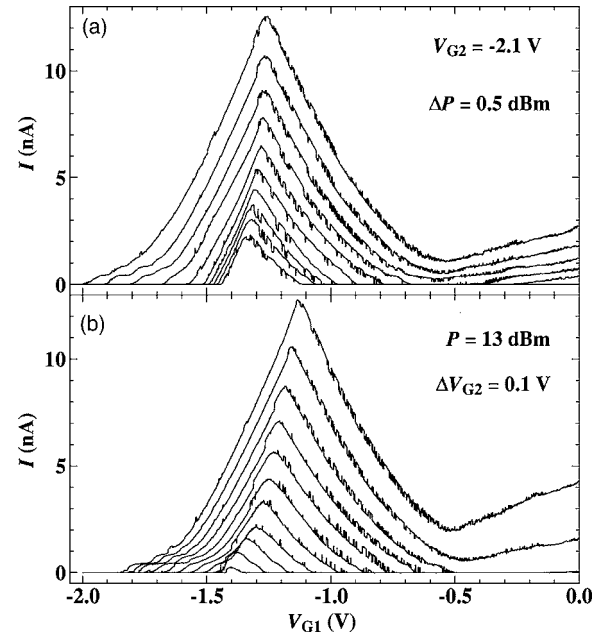


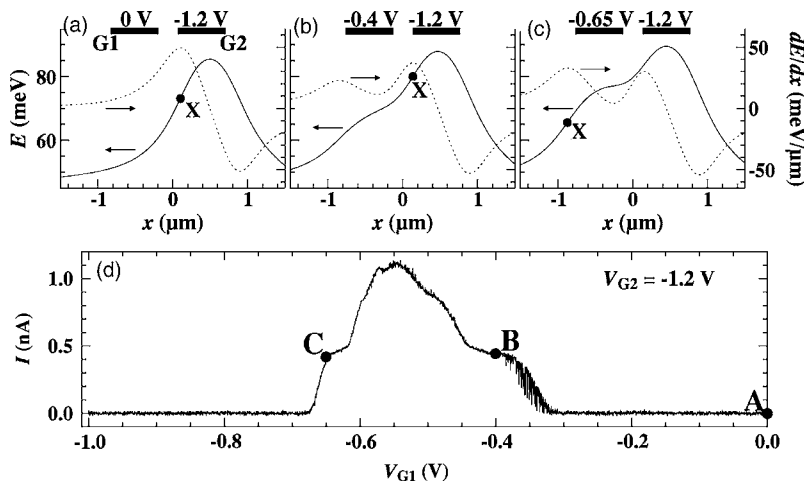
FIG. 3. (a) Transducer power dependence of I - V_{G1} curve. The output power of the signal generator is incremented from 9 dBm (bottom curve) to 13.5 dBm (top curve) by 0.5 dBm, with the voltages on G2 and G3 fixed at -2.1 V and -1.35 V, respectively. (b) V_{G2} dependence of I - V_{G1} curve. V_{G2} is decremented from -2 V (top curve) to -3 V (bottom curve) by 0.1 V steps. The transducer power is set at 13 dBm, and the voltage on G3 is -1.35 V.

nel due to additional contribution by the negative voltage on G2. When V_{G2} reaches ~ -0.3 V, however, the current shows a maximum around $V_{G1} = -0.4$ V, and starts to decrease as V_{G1} is swept more positive. When $V_{G2} \sim -1$ V, the current eventually decreases to zero, showing another set of plateaux. The quantized values of these plateaux match those of the original current-quantization plateaux (on the left-hand side of the current peak). As V_{G2} is made more negative, the peak value of the current decreases. When $V_{G2} = -1.3$ V (the third curve from the bottom), the ef plateau on the left-hand side of the peak merges with that on the right-hand side of the peak, showing a single long plateau (although it is not completely flat).

One interesting way to view the data is to start from $V_{G1}=0$ V when $V_{G2} \sim -1.2$ V. The current is initially zero as G2 completely shuts off the acoustoelectric current. Then, counterintuitively, applying negative voltage to G1 opens up the channel and the current starts to flow, showing first the ef plateau, and then the $2ef$ plateau. Eventually, the channel starts to close, showing the current plateaux again on the way down.

Changing the transducer power has a similar effect on the I - V_{G1} curve as changing V_{G2} (see Fig. 3). Figure 3(a) shows the power dependence as the output of the signal generator is incremented from 9 dBm to 13.5 dBm when V_{G2} is fixed at -2.1 V. Figure 3(b) shows V_{G2} dependence, as V_{G2} is decremented from -2 V to -3 V with a constant $P=13$ dBm. The voltage on G3 is -1.35 V for both cases. The sharp current peaks suggest a sudden transition in the system.

We found that this puzzling behavior can be understood if



we consider that the acoustoelectric current is limited by the maximum potential slope at the entrance of the channel. We calculate the channel potential by solving three-dimensional Laplace's equation with the method given in Ref. 13. We opt for Laplace's equation as a good approximation, rather than Poisson's equation, because the channel is almost depleted except for the insignificant number of electrons transported by the SAW. Figures 4(a)–4(c) show the calculated potential energy along the channel (in the SAW traveling direction x) with three cases of V_{G1} and V_{G2} . Here, SAWs travel from left to right. Figure 4(d) plots the data with $V_{G2} = -1.2\text{ V}$ in Fig. 2. When $V_{G1} = 0\text{ V}$ [Fig. 4(a)], the steepest point of the potential (marked by "X") is just on the left of G2. This is where the SAW confinement potential is the weakest, and the last excess electron falls out from each SAW potential minimum to the source 2DEG, according to the model by Robinson and Barnes.⁹ From this point to the right, electrons cannot escape from the potential minimum until they reach the other side of the channel, where they will go to the drain 2DEG.

When a small negative voltage is applied to G1, the maximum potential slope becomes shallower as shown in Fig. 4(b). This results in more electrons being accommodated in the SAW minima, and hence the acoustoelectric current recovers. As V_{G1} is made more negative, the potential slope becomes even shallower, and more current flows. Eventually, the potential slope on the left of G1 [marked by "X" in Fig. 4(c)] becomes steeper than the original point. Then, the current starts to decrease as V_{G1} is swept further. The peak in the I - V_{G1} curve marks the voltage when the point of maximum potential gradient switches between the two spatially different positions. As a change in the potential at one point tries to increase the current and the other tries to decrease it, switching between the two points causes a sudden transition in the current, appearing as a sharp peak. This interpretation is consistent with the fact that the frequency of the random-telegraph-signal (RTS) noise abruptly changes between the left- and right-hand side of the peak. RTS noise is caused by local charge centers and it is likely that different charge centers with different frequencies would affect the two different locations for the maximum electric field. Although we do not claim our calculation to be accurate, we note that, according to the calculation, the current peak should occur at -0.61 V ,

FIG. 4. (a)–(c) Three cases of the potential energy at the center of the channel (450 nm away from G3) in the SAW traveling direction x : (a) $V_{G1} = 0\text{ V}$, (b) $V_{G1} = -0.4\text{ V}$, and (c) $V_{G1} = -0.65\text{ V}$. $V_{G2} = -1.2\text{ V}$ for all the cases. Solid lines are the potential from the three-dimensional solution of Laplace's equation, and their derivatives (i.e., proportional to the electric field) are plotted with the dotted line. The steepest part of the potential is marked by "X." The SAW travels from left to right. (d) The experimental curve in Fig. 2 with $V_{G2} = -1.2\text{ V}$. Points "A," "B," and "C" mark the voltages corresponding to (a), (b), and (c), respectively.

which is in a reasonable agreement with the experimental value of -0.55 V .

In Figs. 5(a) and 5(c), we plot the calculated peak position as solid lines for the data shown in Fig. 3. In the case of constant V_{G2} with P varied [Fig. 5(a)], the calculation predicts that the current peak should be at a fixed position. Although the experimental values [crosses in Fig. 5(a)] are approximately 30% larger than the calculation, they are qualitatively in agreement on the point that their position in V_{G1} barely changes. On the other hand, when V_{G2} is varied, the current-peak position moves accordingly as shown in

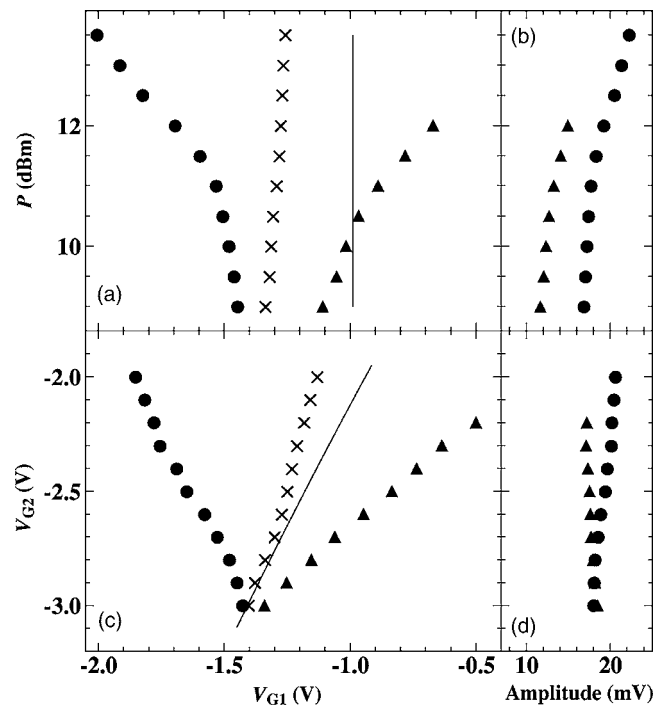


FIG. 5. (a) The positions in V_{G1} of the current peak (crosses), the pinch off on the left of the peak (circles), and that on the right of the peak (triangles) of the data shown in Fig. 3(a). The solid line is the theoretical position of the current peak. (b) SAW amplitude (peak to peak) derived from the calculated potential at the pinch off (see text for detail). (c) and (d) Similar plots for the data in Fig. 3(b).

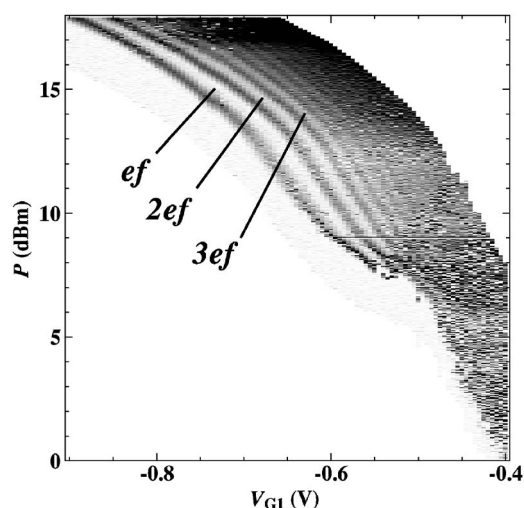


FIG. 6. Grayscale plot of the power dependence of the acoustoelectric current. Here, the transducer power P is swept, instead of gate voltage, to average out sample heating. V_{G1} is incremented by 5 mV. The derivative of the curve is plotted in grayscale with white representing plateaux. Up to five current-quantization plateaux can be seen. For $P \leq 7$ dBm, random-telegraph-signal noise becomes dominant. The data were not taken in the blank region on the top-right and bottom-left corners.

Fig. 5(c). Here, the experiment matches the calculation reasonably well.

These experimental results seem to be inconsistent with the transport mechanism by turnstile motion of a quantum dot proposed by Fletcher *et al.*,¹⁰ as it cannot explain the increase in the acoustoelectric current when the gate is swept to more negative voltage (because the potential of the quantum dot should always increase). However, this inconsistency may be due to the difference in the SAW amplitude used in the two experiments. The transducer power used in the work by Fletcher *et al.* is significantly smaller (-30 to 0 dBm), although a direct comparison is difficult because of different experimental parameters such as the trans-

ducer efficiency and attenuation in the wire. From the Coulomb-blockade picture, they estimate the SAW amplitude to be around 1 mV. We estimate our SAW amplitude in Figs. 5(b) and 5(d) by assuming that, at the pinch-off voltage, the maximum SAW field matches the maximum potential gradient so that the confinement is broken.¹⁴ The estimated SAW amplitude is an order of magnitude larger than that by Fletcher *et al.*¹⁰

Figure 6 shows the power dependence of acoustoelectric current of our device. There was too much RTS noise in the curves below $P \sim 7$ dBm, and none of the fan structure observed by Fletcher *et al.*¹⁰ can be seen. It is very plausible that the system switches between the two pictures as the transducer power is varied. In this regard, it would be interesting to conduct similar measurements at low power on a sample that does not display RTS noise, in order to investigate whether similar current peak appears in the region where the quantum-dot picture seems to apply.

In summary, we have investigated acoustoelectric current through a channel defined by two side gates in series. When the second gate is set past the pinch-off voltage, sweeping the first gate to negative voltage recovers the current, showing quantization plateaux. The current eventually decreases to zero as another set of quantized plateaux appear. We have explained this behavior by considering that the acoustoelectric current is limited by the steepest part of the potential slope, in agreement with the classical model given by Robinson and Barnes.⁹ This suggests that suppressing the thermal excitation of the electrons confined in SAW potential is a key to improve the current-quantization accuracy. We also compared this interpretation with the quantum-dot picture by Fletcher *et al.*, and suggest that the SAW transport mechanism is dependent on the SAW amplitude.

This research is part of QIP IRC www.qipirc.org (GR/S82176/01) and is also supported by the UK EPSRC. The authors thank A. M. Robinson, J. Cunningham, J. Ebbecke, and V. I. Talyanskii for useful discussions. One of the authors (M.K.) also acknowledges financial support from the Cambridge-MIT Institute.

¹J. M. Shilton, V. I. Talyanskii, M. Pepper, D. A. Ritchie, J. E. F. Frost, C. J. B. Ford, C. G. Smith, and G. A. C. Jones, *J. Phys.: Condens. Matter* **8**, L531 (1996).

²T. J. M. Janssen and A. Hartland, *Physica B* **284–288**, 1790 (2000).

³C. H. W. Barnes, J. M. Shilton, and A. M. Robinson, *Phys. Rev. B* **62**, 8410 (2000).

⁴C. H. W. Barnes, *Philos. Trans. R. Soc. London, Ser. A* **361**, 1487 (2003).

⁵K. Flensberg, Q. Niu, and M. Pustilnik, *Phys. Rev. B* **60**, R16291 (1999).

⁶P. A. Maksym, *Phys. Rev. B* **61**, 4727 (2000).

⁷G. R. Aizin, G. Gumbs, and M. Pepper, *Phys. Rev. B* **58**, 10589 (1998).

⁸G. Gumbs, G. R. Aizin, and M. Pepper, *Phys. Rev. B* **60**, R13954 (1999).

⁹A. M. Robinson and C. H. W. Barnes, *Phys. Rev. B* **63**, 165418

(2001).

¹⁰N. E. Fletcher, J. Ebbecke, T. J. B. M. Janssen, F. J. Ahlers, M. Pepper, H. E. Beere, and D. A. Ritchie, *Phys. Rev. B* **68**, 245310 (2003).

¹¹L. P. Kouwenhoven, A. T. Johnson, N. C. van der Vaart, C. J. P. M. Harmans, and C. T. Foxon, *Phys. Rev. Lett.* **67**, 1626 (1991).

¹²At $V_{G1}=V_{G2}=0$, there is no lateral confinement, and the SAW does not drive an acoustoelectric current since the extent of the 2DEG is wider than the SAW beam. The offset voltage on the current preamplifier affects measurements when the channel is not pinched off, which is the upper right-hand side of Fig. 2, but not in the region where ef plateaux are observed.

¹³J. H. Davies, I. A. Larkin, and E. V. Sukhorukov, *J. Appl. Phys.* **77**, 4504 (1995).

¹⁴We note that this is an approximation since a finite zero-point energy of the confinement potential may affect the pinch-off voltage.